FERMILAB-Pub-04/225-E

Measurement of the B_s^0 lifetime in the exclusive decay channel $B_s^0 \to J/\psi\phi$

V.M. Abazov,[33] B. Abbott,[70] M. Abolins,[61] B.S. Acharya,[27] D.L. Adams,[68] M. Adams,[48] T. Adams,[46] M. Agelou,[17] J.-L. Agram,[18] S.N. Ahmed,[32] S.H. Ahn,[29] G.D. Alexeev,[33] G. Alkhazov,[37] A. Alton,[60] G. Alverson,[59] G.A. Alves,[2] M. Anastasoaie,[32] S. Anderson,[42] B. Andrieu,[16] Y. Arnoud,[13] A. Askew,[73] B. Åsman,[38] O. Atramentov,[53] C. Autermann,[20] C. Avila,[7] L. Babukhadia,[67] T.C. Bacon,[40] F. Badaud,[12] A. Baden,[57] S. Baffioni,[14] B. Baldin,[47] P.W. Balm,[31] S. Banerjee,[27] E. Barberis,[59] P. Bargassa,[73] P. Baringer,[54] C. Barnes,[40] J. Barreto,[2] J.F. Bartlett,[47] U. Bassler,[16] D. Bauer,[51] A. Bean,[54] S. Beauceron,[16] F. Beaudette,[15] M. Begel,[66] A. Bellavance,[63] S.B. Beri,[26] G. Bernardi,[16] R. Bernhard,[47,*] I. Bertram,[39] M. Besançon,[17] A. Besson,[18] R. Beuselinck,[40] V.A. Bezzubov,[36] P.C. Bhat,[47] V. Bhatnagar,[26] M. Bhattacharjee,[67] M. Binder,[24] A. Bischoff,[45] K.M. Black,[58] I. Blackler,[40] G. Blazey,[49] F. Blekman,[31] S. Blessing,[46] D. Bloch,[18] U. Blumenschein,[22] A. Boehnlein,[47] O. Boeriu,[52] T.A. Bolton,[55] P. Bonamy,[17] F. Borcherding,[47] G. Borissov,[39] K. Bos,[31] T. Bose,[65] C. Boswell,[45] A. Brandt,[72] G. Briskin,[71] R. Brock,[61] G. Brooijmans,[65] A. Bross,[47] N.J. Buchanan,[46] D. Buchholz,[50] M. Buehler,[48] V. Buescher,[22] S. Burdin,[47] T.H. Burnett,[75] E. Busato,[16] J.M. Butler,[58] J. Bystricky,[17] F. Canelli,[66] W. Carvalho,[3] B.C.K. Casey,[71] D. Casey,[61] N.M. Cason,[52] H. Castilla-Valdez,[30] S. Chakrabarti,[27] D. Chakraborty,[49] K.M. Chan,[66] A. Chandra,[27] D. Chapin,[71] F. Charles,[18] E. Cheu,[42] L. Chevalier,[17] D.K. Cho,[66] S. Choi,[45] S. Chopra,[68] T. Christiansen,[24] L. Christofek,[54] D. Claes,[63] A.R. Clark,[43] B. Clément,[18] C. Clément,[38] Y. Coadou,[5] D.J. Colling,[40] L. Coney,[52] B. Connolly,[46] M. Cooke,[73] W.E. Cooper,[47] D. Coppage,[54] M. Corcoran,[73] J. Coss,[19] A. Cothenet,[14] M.-C. Cousinou,[14] S. Crépé-Renaudin,[13] M. Cristetiu,[45] M.A.C. Cummings,[49] D. Cutts,[71] H. da Motta,[2] B. Davies,[39] G. Davies,[40] G.A. Davis,[50] K. De,[72] P. de Jong,[31] S.J. de Jong,[32] E. De La Cruz-Burelo,[30] C. De Oliveira Martins,[3] S. Dean,[41] K. Del Signore,[60] F. Déliot,[17] P.A. Delsart,[19] M. Demarteau,[47] R. Demina,[66] P. Demine,[17] D. Denisov,[47] S.P. Denisov,[36] S. Desai,[67] H.T. Diehl,[47] M. Diesburg,[47] M. Doidge,[39] H. Dong,[67] S. Doulas,[59] L. Duflot,[15] S.R. Dugad,[27] A. Duperrin,[14] J. Dyer,[61] A. Dyshkant,[49] M. Eads,[49] D. Edmunds,[61] T. Edwards,[41] J. Ellison,[45] J. Elmsheuser,[24] J.T. Eltzroth,[72] V.D. Elvira,[47] S. Eno,[57] P. Ermolov,[35] O.V. Eroshin,[36] J. Estrada,[47] D. Evans,[40] H. Evans,[65] A. Evdokimov,[34] V.N. Evdokimov,[36] J. Fast,[47] S.N. Fatakia,[58] D. Fein,[42] L. Feligioni,[58] T. Ferbel,[66] F. Fiedler,[24] F. Filthaut,[32] W. Fisher,[64] H.E. Fisk,[47] F. Fleuret,[16] M. Fortner,[49] H. Fox,[22] W. Freeman,[47] S. Fu,[47] S. Fuess,[47] C.F. Galea,[32] E. Gallas,[47] E. Galyaev,[52] M. Gao,[65] C. Garcia,[66] A. Garcia-Bellido,[75] J. Gardner,[54] V. Gavrilov,[34] P. Gay,[12] D. Gelé,[18] R. Gelhaus,[45] K. Genser,[47] C.E. Gerber,[48] Y. Gershtein,[71] G. Geurkov,[71] G. Ginther,[66] K. Goldmann,[25] T. Golling,[21] B. Gómez,[7] K. Gounder,[47] A. Goussiou,[52] G. Graham,[57] P.D. Grannis,[67] S. Greder,[18] J.A. Green,[53] H. Greenlee,[47] Z.D. Greenwood,[56] E.M. Gregores,[4] S. Grinstein,[1] Ph. Gris,[12] J.-F. Grivaz,[15] L. Groer,[65] S. Grünendahl,[47] M.W. Grünewald,[28] W. Gu,[6] S.N. Gurzhiev,[36] G. Gutierrez,[47] P. Gutierrez,[70] A. Haas,[65] N.J. Hadley,[57] H. Haggerty,[47] S. Hagopian,[46] I. Hall,[70] R.E. Hall,[44] C. Han,[60] L. Han,[41] K. Hanagaki,[47] P. Hanlet,[72] K. Harder,[55] R. Harrington,[59] J.M. Hauptman,[53] R. Hauser,[61] C. Hays,[65] J. Hays,[50] T. Hebbeker,[20] C. Hebert,[54] D. Hedin,[49] J.M. Heinmiller,[48] A.P. Heinson,[45] U. Heintz,[58] C. Hensel,[54] G. Hesketh,[59] M.D. Hildreth,[52] R. Hirosky,[74] J.D. Hobbs,[67] B. Hoeneisen,[11] M. Hohlfeld,[23] S.J. Hong,[29] R. Hooper,[71] S. Hou,[60] P. Houben,[31] Y. Hu,[67] J. Huang,[51] Y. Huang,[60] I. Iashvili,[45] R. Illingworth,[47] A.S. Ito,[47] S. Jabeen,[54] M. Jaffré,[15] S. Jain,[70] V. Jain,[68] K. Jakobs,[22] A. Jenkins,[40] R. Jesik,[40] Y. Jiang,[60] K. Johns,[42] M. Johnson,[47] P. Johnson,[42] A. Jonckheere,[47] P. Jonsson,[40] H. Jöstlein,[47] A. Juste,[47] M.M. Kado,[43] D. Käfer,[20] W. Kahl,[55] S. Kahn,[68] E. Kajfasz,[14] A.M. Kalinin,[33] J. Kalk,[61] D. Karmanov,[35] J. Kasper,[58] D. Kau,[46] Z. Ke,[6] R. Kehoe,[61] S. Kermiche,[14] S. Kesisoglou,[71] A. Khanov,[66] A. Kharchilava,[52] Y.M. Kharzheev,[33] K.H. Kim,[29] B. Klima,[47] M. Klute,[21] J.M. Kohli,[26] M. Kopal,[70] V.M. Korablev,[36] J. Kotcher,[68] B. Kothari,[65] A.V. Kotwal,[65] A. Koubarovsky,[35] O. Kouznetsov,[13] A.V. Kozelov,[36] J. Kozminski,[61] J. Krane,[53] M.R. Krishnaswamy,[27] S. Krzywdzinski,[47] M. Kubantsev,[55] S. Kuleshov,[34] Y. Kulik,[47] S. Kunori,[57] A. Kupco,[17] T. Kurča,[19] V.E. Kuznetsov,[45] S. Lager,[38] N. Lahrichi,[17] G. Landsberg,[71] J. Lazoflores,[46] A.-C. Le Bihan,[18] P. Lebrun,[19] S.W. Lee,[29] W.M. Lee,[46] A. Leflat,[35] C. Leggett,[43] F. Lehner,[47,*] C. Leonidopoulos,[65] P. Lewis,[40] J. Li,[72] Q.Z. Li,[47] X. Li,[6] J.G.R. Lima,[49] D. Lincoln,[47] S.L. Linn,[46] J. Linnemann,[61] V.V. Lipaev,[36] R. Lipton,[47] L. Lobo,[40] A. Lobodenko,[37] M. Lokajicek,[10] A. Lounis,[18] J. Lu,[6] H.J. Lubatti,[75] A. Lucotte,[13] L. Lueking,[47] C. Luo,[51] M. Lynker,[52] A.L. Lyon,[47] A.K.A. Maciel,[49] R.J. Madaras,[43] P. Mättig,[25] A. Magerkurth,[60] A.-M. Magnan,[13] M. Maity,[58] N. Makovec,[15] P.K. Mal,[27] S. Malik,[56] V.L. Malyshev,[33] V. Manankov,[35] H.S. Mao,[6] Y. Maravin,[47] T. Marshall,[51] M. Martens,[47] M.I. Martin,[49]

S.E.K. Mattingly,[71] A.A. Mayorov,[36] R. McCarthy,[67] R. McCroskey,[42] T. McMahon,[69] D. Meder,[23] H.L. Melanson,[47] A. Melnitchouk,[62] X. Meng,[6] M. Merkin,[35] K.W. Merritt,[47] A. Meyer,[20] C. Miao,[71] H. Miettinen,[73] D. Mihalcea,[49] J. Mitrevski,[65] N. Mokhov,[47] J. Molina,[3] N.K. Mondal,[27] H.E. Montgomery,[47] R.W. Moore,[5] M. Mostafa,[1] G.S. Muanza,[19] M. Mulders,[47] Y.D. Mutaf,[67] E. Nagy,[14] F. Nang,[42] M. Narain,[58] V.S. Narasimham,[27] N.A. Naumann,[32] H.A. Neal,[60] J.P. Negret,[7] S. Nelson,[46] P. Neustroev,[37] C. Noeding,[22] A. Nomerotski,[47] S.F. Novaes,[4] T. Nunnemann,[24] E. Nurse,[41] V. O'Dell,[47] D.C. O'Neil,[5] V. Oguri,[3] N. Oliveira,[3] B. Olivier,[16] N. Oshima,[47] G.J. Otero y Garzón,[48] P. Padley,[73] K. Papageorgiou,[48] N. Parashar,[56] J. Park,[29] S.K. Park,[29] J. Parsons,[65] R. Partridge,[71] N. Parua,[67] A. Patwa,[68] P.M. Perea,[45] E. Perez,[17] O. Peters,[31] P. Pétroff,[15] M. Petteni,[40] L. Phaf,[31] R. Piegaia,[1] P.L.M. Podesta-Lerma,[30] V.M. Podstavkov,[47] Y. Pogorelov,[52] B.G. Pope,[61] E. Popkov,[58] W.L. Prado da Silva,[3] H.B. Prosper,[46] S. Protopopescu,[68] M.B. Przybycien,[50,†] J. Qian,[60] A. Quadt,[21] B. Quinn,[62] K.J. Rani,[27] P.A. Rapidis,[47] P.N. Ratoff,[39] N.W. Reay,[55] J.-F. Renardy,[17] S. Reucroft,[59] J. Rha,[45] M. Ridel,[15] M. Rijssenbeek,[67] I. Ripp-Baudot,[18] F. Rizatdinova,[55] C. Royon,[17] P. Rubinov,[47] R. Ruchti,[52] B.M. Sabirov,[33] G. Sajot,[13] A. Sánchez-Hernández,[30] M.P. Sanders,[41] A. Santoro,[3] G. Savage,[47] L. Sawyer,[56] T. Scanlon,[40] R.D. Schamberger,[67] H. Schellman,[50] P. Schieferdecker,[24] C. Schmitt,[25] A.A. Schukin,[36] A. Schwartzman,[64] R. Schwienhorst,[61] S. Sengupta,[46] H. Severini,[70] E. Shabalina,[48] V. Shary,[17] W.D. Shephard,[52] D. Shpakov,[59] R.A. Sidwell,[55] V. Simak,[9] V. Sirotenko,[47] D. Skow,[47] P. Skubic,[70] P. Slattery,[66] R.P. Smith,[47] K. Smolek,[9] G.R. Snow,[63] J. Snow,[69] S. Snyder,[68] S. Söldner-Rembold,[41] X. Song,[49] Y. Song,[72] L. Sonnenschein,[58] A. Sopczak,[39] V. Sorín,[1] M. Sosebee,[72] K. Soustruznik,[8] M. Souza,[2] B. Spurlock,[72] N.R. Stanton,[55] J. Stark,[13] J. Steele,[56] G. Steinbrück,[65] K. Stevenson,[51] V. Stolin,[34] A. Stone,[48] D.A. Stoyanova,[36] J. Strandberg,[38] M.A. Strang,[72] M. Strauss,[70] R. Ströhmer,[24] M. Strovink,[43] L. Stutte,[47] S. Sumowidagdo,[46] A. Sznajder,[3] M. Talby,[14] P. Tamburello,[42] W. Taylor,[67] P. Telford,[41] J. Temple,[42] S. Tentindo-Repond,[46] E. Thomas,[14] B. Thooris,[17] M. Tomoto,[47] T. Toole,[57] J. Torborg,[52] S. Towers,[67] T. Trefzger,[23] S. Trincaz-Duvoid,[16] T.G. Trippe,[43] B. Tuchming,[17] C. Tully,[64] A.S. Turcot,[68] P.M. Tuts,[65] L. Uvarov,[37] S. Uvarov,[37] S. Uzunyan,[49] B. Vachon,[47] R. Van Kooten,[51] W.M. van Leeuwen,[31] N. Varelas,[48] E.W. Varnes,[42] I.A. Vasilyev,[36] M. Vaupel,[25] P. Verdier,[15] L.S. Vertogradov,[33] M. Verzocchi,[57] F. Villeneuve-Seguier,[40] J.-R. Vlimant,[16] E. Von Toerne,[55] M. Vreeswijk,[31] T. Vu Anh,[15] H.D. Wahl,[46] R. Walker,[40] N. Wallace,[42] Z.-M. Wang,[67] J. Warchol,[52] M. Warsinsky,[21] G. Watts,[75] M. Wayne,[52] M. Weber,[47] H. Weerts,[61] M. Wegner,[20] N. Wermes,[21] A. White,[72] V. White,[47] D. Whiteson,[43] D. Wicke,[47] D.A. Wijngaarden,[32] G.W. Wilson,[54] S.J. Wimpenny,[45] J. Wittlin,[58] T. Wlodek,[72] M. Wobisch,[47] J. Womersley,[47] D.R. Wood,[59] Z. Wu,[6] T.R. Wyatt,[41] Q. Xu,[60] N. Xuan,[52] R. Yamada,[47] M. Yan,[57] T. Yasuda,[47] Y.A. Yatsunenko,[33] Y. Yen,[25] K. Yip,[68] S.W. Youn,[50] J. Yu,[72] A. Yurkewicz,[61] A. Zabi,[15] A. Zatserklyaniy,[49] M. Zdrazil,[67] C. Zeitnitz,[23] B. Zhang,[6] D. Zhang,[47] X. Zhang,[70] T. Zhao,[75] Z. Zhao,[60] H. Zheng,[52] B. Zhou,[60] Z. Zhou,[53] J. Zhu,[57] M. Zielinski,[66] D. Zieminska,[51] A. Zieminski,[51] R. Zitoun,[67] V. Zutshi,[49] E.G. Zverev,[35] and A. Zylberstejn[17]

(DØ Collaboration)

[1] *Universidad de Buenos Aires, Buenos Aires, Argentina*
[2] *LAFEX, Centro Brasileiro de Pesquisas Físicas, Rio de Janeiro, Brazil*
[3] *Universidade do Estado do Rio de Janeiro, Rio de Janeiro, Brazil*
[4] *Instituto de Física Teórica, Universidade Estadual Paulista, São Paulo, Brazil*
[5] *University of Alberta, Edmonton, Canada and Simon Fraser University, Burnaby, Canada*
[6] *Institute of High Energy Physics, Beijing, People's Republic of China*
[7] *Universidad de los Andes, Bogotá, Colombia*
[8] *Charles University, Center for Particle Physics, Prague, Czech Republic*
[9] *Czech Technical University, Prague, Czech Republic*
[10] *Institute of Physics, Academy of Sciences, Center for Particle Physics, Prague, Czech Republic*
[11] *Universidad San Francisco de Quito, Quito, Ecuador*
[12] *Laboratoire de Physique Corpusculaire, IN2P3-CNRS, Université Blaise Pascal, Clermont-Ferrand, France*
[13] *Laboratoire de Physique Subatomique et de Cosmologie, IN2P3-CNRS, Universite de Grenoble 1, Grenoble, France*
[14] *CPPM, IN2P3-CNRS, Université de la Méditerranée, Marseille, France*
[15] *Laboratoire de l'Accélérateur Linéaire, IN2P3-CNRS, Orsay, France*
[16] *LPNHE, Universités Paris VI and VII, IN2P3-CNRS, Paris, France*
[17] *DAPNIA/Service de Physique des Particules, CEA, Saclay, France*
[18] *IReS, IN2P3-CNRS, Université Louis Pasteur, Strasbourg, France and Université de Haute Alsace, Mulhouse, France*
[19] *Institut de Physique Nucléaire de Lyon, IN2P3-CNRS, Université Claude Bernard, Villeurbanne, France*
[20] *RWTH Aachen, III. Physikalisches Institut A, Aachen, Germany*
[21] *Universität Bonn, Physikalisches Institut, Bonn, Germany*
[22] *Universität Freiburg, Physikalisches Institut, Freiburg, Germany*

[23] *Universität Mainz, Institut für Physik, Mainz, Germany*
[24] *Ludwig-Maximilians-Universität München, München, Germany*
[25] *Fachbereich Physik, University of Wuppertal, Wuppertal, Germany*
[26] *Panjab University, Chandigarh, India*
[27] *Tata Institute of Fundamental Research, Mumbai, India*
[28] *University College Dublin, Dublin, Ireland*
[29] *Korea Detector Laboratory, Korea University, Seoul, Korea*
[30] *CINVESTAV, Mexico City, Mexico*
[31] *FOM-Institute NIKHEF and University of Amsterdam/NIKHEF, Amsterdam, The Netherlands*
[32] *University of Nijmegen/NIKHEF, Nijmegen, The Netherlands*
[33] *Joint Institute for Nuclear Research, Dubna, Russia*
[34] *Institute for Theoretical and Experimental Physics, Moscow, Russia*
[35] *Moscow State University, Moscow, Russia*
[36] *Institute for High Energy Physics, Protvino, Russia*
[37] *Petersburg Nuclear Physics Institute, St. Petersburg, Russia*
[38] *Lund University, Lund, Sweden, Royal Institute of Technology and Stockholm University, Stockholm, Sweden and Uppsala University, Uppsala, Sweden*
[39] *Lancaster University, Lancaster, United Kingdom*
[40] *Imperial College, London, United Kingdom*
[41] *University of Manchester, Manchester, United Kingdom*
[42] *University of Arizona, Tucson, Arizona 85721*
[43] *Lawrence Berkeley National Laboratory and University of California, Berkeley, California 94720*
[44] *California State University, Fresno, California 93740*
[45] *University of California, Riverside, California 92521*
[46] *Florida State University, Tallahassee, Florida 32306*
[47] *Fermi National Accelerator Laboratory, Batavia, Illinois 60510*
[48] *University of Illinois at Chicago, Chicago, Illinois 60607*
[49] *Northern Illinois University, DeKalb, Illinois 60115*
[50] *Northwestern University, Evanston, Illinois 60208*
[51] *Indiana University, Bloomington, Indiana 47405*
[52] *University of Notre Dame, Notre Dame, Indiana 46556*
[53] *Iowa State University, Ames, Iowa 50011*
[54] *University of Kansas, Lawrence, Kansas 66045*
[55] *Kansas State University, Manhattan, Kansas 66506*
[56] *Louisiana Tech University, Ruston, Louisiana 71272*
[57] *University of Maryland, College Park, Maryland 20742*
[58] *Boston University, Boston, Massachusetts 02215*
[59] *Northeastern University, Boston, Massachusetts 02115*
[60] *University of Michigan, Ann Arbor, Michigan 48109*
[61] *Michigan State University, East Lansing, Michigan 48824*
[62] *University of Mississippi, University, Mississippi 38677*
[63] *University of Nebraska, Lincoln, Nebraska 68588*
[64] *Princeton University, Princeton, New Jersey 08544*
[65] *Columbia University, New York, New York 10027*
[66] *University of Rochester, Rochester, New York 14627*
[67] *State University of New York, Stony Brook, New York 11794*
[68] *Brookhaven National Laboratory, Upton, New York 11973*
[69] *Langston University, Langston, Oklahoma 73050*
[70] *University of Oklahoma, Norman, Oklahoma 73019*
[71] *Brown University, Providence, Rhode Island 02912*
[72] *University of Texas, Arlington, Texas 76019*
[73] *Rice University, Houston, Texas 77005*
[74] *University of Virginia, Charlottesville, Virginia 22901*
[75] *University of Washington, Seattle, Washington 98195*

(Dated: December 10, 2004)

Using the exclusive decay $B_s^0 \to J/\psi(\mu^+\mu^-)\phi(K^+K^-)$, we report the most precise single measurement of the B_s^0 lifetime. The data sample corresponds to an integrated luminosity of approximately 220 pb^{-1} collected with the DØ detector at the Fermilab Tevatron Collider in 2002–2004. We reconstruct 337 signal candidates, from which we extract the B_s^0 lifetime, $\tau(B_s^0) = 1.444^{+0.098}_{-0.090}\,(\text{stat}) \pm 0.020\,(\text{sys})$ ps. We also report a measurement for the lifetime of the B^0 meson using the exclusive decay $B^0 \to J/\psi(\mu^+\mu^-)K^{*0}(892)(K^+\pi^-)$. We reconstruct 1370 signal candidates, obtaining $\tau(B^0) = 1.473^{+0.052}_{-0.050}\,(\text{stat}) \pm 0.023\,(\text{sys})$ ps, and the ratio of lifetimes,

$\tau(B_s^0)/\tau(B^0) = 0.980^{+0.076}_{-0.071}\,(\text{stat}) \pm 0.003\,(\text{sys})$.

PACS numbers: 14.40.Nd, 13.25.Hw

Lifetime differences among hadrons containing b quarks can be used to probe decay mechanisms that go beyond the quark-spectator model [1]. In the charm sector, lifetime differences are quite large [2]; however, in the bottom sector, due to the larger b-quark mass, these differences are expected to be smaller. Phenomenological models predict differences of about 5% between the lifetimes of B^+ and B^0, but no more than 1% between B^0 and B_s^0 lifetimes [1]. These predictions are consistent with previous measurements of B-meson lifetimes [2]. It has also been postulated [3] that the lifetimes of the two CP eigenstates (of the B_s^0-$\bar{B}_s^0$ system) differ. This could be observed as a difference in lifetime between B_s^0 semileptonic decays, which should have an equal mixture of the two CP eigenstates, and the lifetime for $B_s^0 \to J/\psi\phi$, which is expected to be dominated by the CP-even eigenstate [3].

In this Letter, we report a measurement of the lifetime of the B_s^0 meson using the exclusive decay channel $B_s^0 \to J/\psi\phi$, followed by $J/\psi \to \mu^+\mu^-$ and $\phi \to K^+K^-$. The lifetime is extracted using a simultaneous unbinned maximum likelihood fit to masses and proper decay lengths. We also measure the lifetime of the B^0 meson in the exclusive decay[1] $B^0 \to J/\psi\ K^{*0}(892)$, followed by $J/\psi \to \mu^+\mu^-$ and $K^{*0}(892) \to K^+\pi^-$, and extract the ratio of the lifetimes of the B_s^0 and B^0 mesons. The analysis is based on data collected with the DØ detector in Run II of the Fermilab Tevatron Collider during the period September 2002–February 2004, which corresponds to approximately 220 pb^{-1} of $p\bar{p}$ collisions at $\sqrt{s} = 1.96$ TeV.

The DØ detector is described in detail elsewhere [4]. We describe here only the detector components most relevant to this analysis. The central-tracking system consists of a silicon microstrip tracker (SMT) and a central fiber tracker (CFT), both located inside a 2 T superconducting solenoidal magnet [4]. The tracking system and solenoid is surrounded by a liquid argon calorimeter. The SMT has $\approx 800,000$ individual strips, with typical pitch of $50 - 80$ μm, and a design optimized for tracking and vertexing capability for $|\eta| < 3$, where $\eta = -\ln[\tan(\theta/2)]$ is the pseudorapidity and θ is the polar angle measured relative to the proton beam direction. The system has a six-barrel longitudinal structure, each with a set of four layers arranged axially around the beam pipe, and interspersed with sixteen radial disks. The CFT has eight thin coaxial barrels, each supporting two doublets of overlapping scintillating fibers of 0.835 mm diameter, one doublet parallel to the beam axis, and the other alternating by $\pm 3^\circ$ relative to this axis. Light signals are transferred via clear light fibers to solid-state photon counters that have a quantum efficiency of approximately 80%. The muon system resides beyond the calorimeter, and consists of a layer of tracking detectors and scintillation trigger counters before 1.8 T toroidal magnets, followed by two similar layers after the toroids. Muon identification for $|\eta| < 1$ relies on 10 cm wide drift tubes, while 1 cm wide mini-drift tubes are used for $1 < |\eta| < 2$. Coverage for muons is partially compromised at the bottom of the detector where the calorimeter is supported mechanically from the ground. Luminosity is measured using plastic scintillator arrays located in front of the end calorimeter cryostat, covering $2.7 < |\eta| < 4.4$.

The data collection consists of a three-level trigger system, designed to accommodate the high luminosity of Run II. The first level uses information from the tracking, calorimetry, and muon systems to reduce the rate for accepted events to ≈ 1.5 kHz. At the next trigger level, with more refined information, the rate is reduced further to ≈ 800 Hz. The third and final level of the trigger, with access to all of the event information, uses software algorithms and a computing farm and reduces the output rate to ≈ 50 Hz, which is recorded for further analysis. We did not require the presence of any specific trigger in the event selection.

Reconstruction of $B_s^0 \to J/\psi\phi$ candidates requires a pair of oppositely charged muons that are identified by extrapolating charged tracks into the muon system and matching them with hits in the muon system. All charged tracks used in this analysis are required to have at least one hit in the SMT. We require that muon candidates each have a minimum transverse momentum $p_T > 1.5$ GeV/c and that they form a common vertex, according to the algorithm described in Ref. [5], which is based on a fit requiring a χ^2 probability greater than 1%. The dimuon system was required to have an invariant mass between 2.90 and 3.15 GeV/c^2 and transverse momentum above 4.5 GeV/c. The dimuons are then combined with another pair of oppositely charged tracks, each with $p_T > 0.8$ GeV/c, consistent with the decay $\phi \to K^+K^-$. The ϕ candidate was required to have an invariant mass between 1.008 and 1.032 GeV/c^2 and transverse momentum greater than 2 GeV/c. A four-track secondary vertex is fitted to the products of the J/ψ and ϕ decays, and required to have a χ^2 probability of at least 1%. The mass of the J/ψ candidate is constrained in the fit to the world average J/ψ mass of 3.097 GeV/c^2 [2], the constraint does not take into account the uncertainty in

[1] Unless explicitly stated, the appearance of a specific charge state will also imply its charge conjugate throughout this Letter.

the J/ψ mass. The resulting B_s^0 candidate is required to have $p_T > 6.5$ GeV/c. We allow only one B_s^0 candidate per event, and when multiple candidates exist, we choose the one with the best vertex probability. The resulting invariant mass distribution of the J/ψ-ϕ system is shown in Fig. 1(a).

Each primary vertex is reconstructed using tracks and the mean beam-spot position. The latter is determined for every data run, where a typical run lasts several hours. The initial primary vertex seed is constructed using all available tracks; a track is removed when it causes a change of more than 9 units in the χ^2 for a fit to a common vertex. The process is repeated until no more tracks can be removed [5].

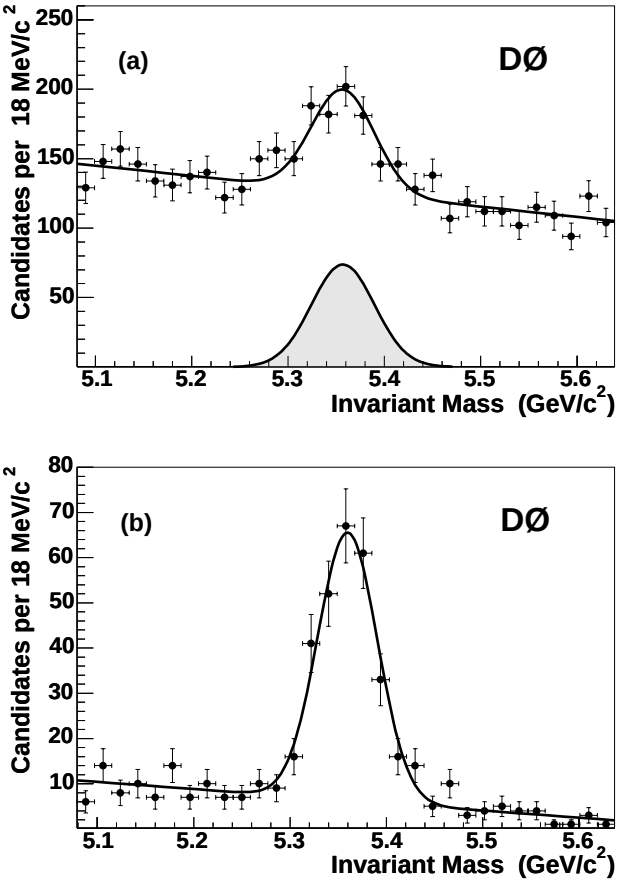

FIG. 1: (a) Mass distribution for B_s^0 candidate events. Points with error bars show the data, and the solid curve represents the result of the fit. The mass distribution for the signal is shown in gray; (b) same distribution after requiring the significance of the lifetime measurement to be $c\tau/\sigma(c\tau) > 5$.

We take the four-track vertex as the position of the secondary vertex. To determine the distance traveled by each B_s^0 candidate, we calculate the signed transverse decay length (in a plane transverse to the direction of the beam), $L_{xy} = \vec{x} \cdot (\vec{p_T}/p_T)$, where $\vec{x}$ is the length vector pointing from the primary to the secondary vertex and $\vec{p_T}$ is the reconstructed transverse momentum vector of the B_s^0. The proper decay length of the B_s^0 candidate is then defined as $c\tau = L_{xy}(M_{B_s^0}/p_T)$, where $M_{B_s^0}$ is taken as the world average mass of the B_s^0 meson 5.3696 GeV/c^2 [2].

Figure 1(b) shows the reconstructed invariant mass distribution of the B_s^0 candidates after a proper decay length significance requirement of $c\tau/\sigma(c\tau) > 5$ is imposed, where $\sigma(c\tau)$ is the uncertainty on $c\tau$. The strong suppression of the background by this cut implies that the background is dominated by zero lifetime vertices, as expected.

The proper decay length (without any restriction on significance) and the invariant mass distributions for candidates passing the above criteria are fit simultaneously using an unbinned maximum likelihood method. The likelihood function $\mathcal{L}$ is given by:

$$\mathcal{L} = \prod_i^N [f_s \mathcal{F}_s^i + (1 - f_s)\mathcal{F}_b^i],$$

where $\mathcal{F}_s$ is the product of probability density functions for mass and proper decay length for B_s^0, $\mathcal{F}_b$ is the equivalent for background, f_s is the fraction of signal, and N is the total number of candidate events in the sample.

The proper decay length for signal events is modeled by a normalized exponential-decay function convoluted with a Gaussian function of width equal to the uncertainty on the proper decay length, which is typically $\approx$ 25 μm. This uncertainty is obtained from the full covariance (error) matrix of tracks at the secondary vertex and the uncertainty in the position of the primary vertex. The uncertainty is multiplied by a scale factor that is a parameter in the fit to allow for a possible misestimate of the decay length uncertainty. The mass distribution of signal events is modeled by a Gaussian function.

The proper decay length for the background is parametrized as a sum of a Gaussian function centered at zero and exponential decay functions, with two short-lived components and a long-lived term. The long-lived component accounts for heavy-flavor backgrounds, while the other terms account for resolution and prompt contributions to background. The mass distribution for the background is modeled by a first-order polynomial.

To determine the background we use a wide mass range of 5.078–5.636 GeV/c^2 in the fit, corresponding to 4236 B_s^0 candidates. The number of background candidates in this range is sufficiently large to measure the parameters of the background with high accuracy and therefore extract a good measurement of the signal fraction and $c\tau(B_s^0)$. The fit provides the $c\tau$ and mass of the B_s^0, the shapes of the proper decay length and mass distributions for the background, and the signal fraction. Table I lists the fit values of the parameters and their uncertainties. The distribution of proper decay length and fits to the B_s^0 candidates are shown in Fig. 2(a).

TABLE I: Values of the extracted mass M_B, resolution on the reconstructed mass σ_M, the measured $c\tau$, the signal fractions f_s, and the scale factor s.

Parameter	$B_s^0 \to J/\psi\phi$ fit values	$B^0 \to J/\psi K^{*0}(892)$ fit values
M_B	5357.0 ± 2.5 MeV/c^2	5271.2 ± 1.5 MeV/c^2
σ_M	$32.9^{+2.5}_{-2.3}$ MeV/c^2	$37.9^{+1.4}_{-1.3}$ MeV/c^2
$c\tau$	433^{+30}_{-27} μm	442^{+16}_{-15} μm
f_s	0.0796 ± 0.0058	0.0446 ± 0.0018
s	1.142 ± 0.028	1.128 ± 0.009

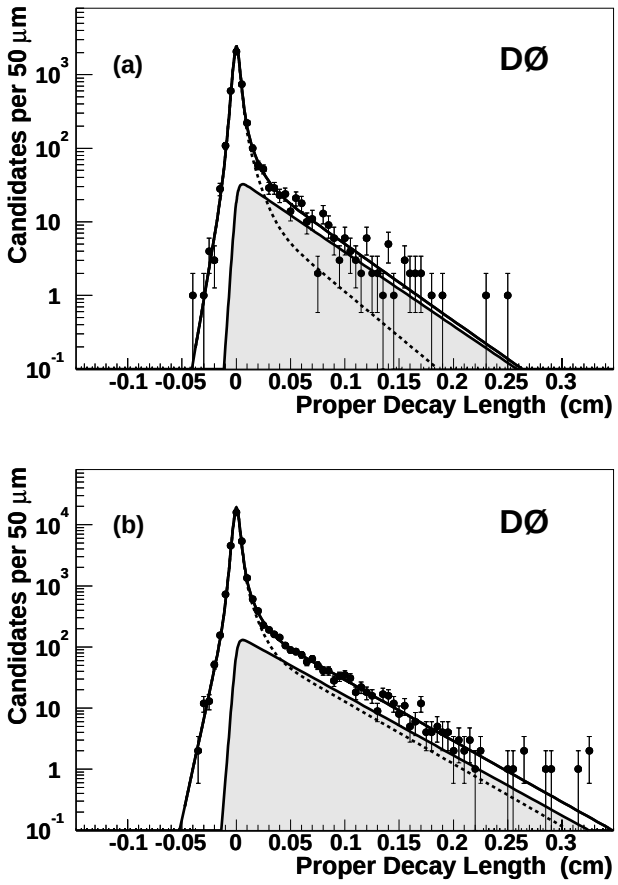

FIG. 2: Proper decay length distributions for (a) B_s^0 and (b) B^0 candidates. The points with error bars show the data. The solid curve shows the total fit, the dashed curve the background component, and the shaded region the signal.

With a very similar four-track topology in the final state, the exclusive decay $B^0 \to J/\psi K^{*0}(892)$ followed by $J/\psi \to \mu^+\mu^-$ and $K^{*0}(892) \to K^+\pi^-$ is reconstructed using the same selection criteria and algorithms as for the B_s^0 channel described above. The only differences are the requirement that the p_T of the pion be greater than 0.5 GeV/c, and the selection of the $K^{*0}(892)$ candidates. The combination of two oppositely charged tracks, assuming the pion mass for one and the kaon mass for the other, that gives an invariant mass closest to the mass of the $K^{*0}(892)$ [2] is selected for further study. The invariant mass of these combinations is required to be between 0.850 and 0.930 GeV/c^2. Using the sample of B^0 candidates in the mass range 4.935–5.610 GeV/c^2, corresponding to 30692 candidates, we determine the $c\tau$ and mass of the B^0 using exactly the same procedure as used for B_s^0 mesons. Results are also given in Table I, and the distribution of proper decay length is shown in Fig. 2(b).

Detailed Monte Carlo studies were performed on ensembles of events comparable to data samples, with similar resolutions, pulls, fitting and selection criteria. No significant biases resulting from our analysis procedures were observed. To test the stability of the fit results for B_s^0 and B^0 mesons, we split each data sample into two roughly equal parts in order to study different kinematic and geometric parameters, compared the fit results, and found consistency within their uncertainties. We varied the selection criteria and mass ranges, and did not observe any significant shifts. Using Monte Carlo samples with different input proper decay lengths in the range 340 to 560 μm, we checked the response of our fits to this variation, and found it to be linear in this range. We studied the contamination of our sample from cross-feed between B_s^0 and B^0 using Monte Carlo events. The estimated contamination is 4.4% for B_s^0 and 1.1% for B^0, with invariant mass spread almost uniformly across the entire mass range. Therefore, their contributions are included in the long-lived heavy-flavor component of the background. To study possible biases from our fitting procedure, we used toy Monte Carlo ensembles with the same statistics as our data and with distributions matching those in data. These samples were fit, and the resulting means and widths of the distributions of extracted parameters are consistent with the fits to data.

Other sources of systematic uncertainty have been considered, and the contributions are listed in Table II. For the B_s^0 lifetime, there are major contributions from determination of the background, the model for resolution, and the reconstruction of the secondary vertex. To determine the systematic error due to the uncertainty in the background, we considered different models for the mass and decay-length distributions. In particular, to account for any model dependence on the invariant mass of misreconstructed heavy-flavor hadrons, we fit the probability distributions separately in the lower-mass and higher-mass side-band regions, and found the long-lived component to have different exponents. Combining the two lifetime values for the long-lived components, we modified the functional form of the long-lived component for the global background in our fit. The two long-lived components were combined using a weighting parameter $w = 0.98^{+0.02}_{-0.36}$. This weighting parameter was varied by its uncertainty. The largest difference in the $c\tau(B_s^0)$ observed in these variations of background modeling was

found to be 4 μm, and is taken as the systematic uncertainty due to this source. The effect of uncertainty in the proper decay length resolution was studied by using an alternative resolution function consisting of two Gaussian functions (with the same mean but different width), resulting in a difference in the fitted $c\tau(B_s^0)$ of 3 μm. Uncertainty or biases in the determination of the secondary vertex were estimated using secondary vertices constructed with the J/ψ tracks only, resulting in a $c\tau(B_s^0)$ shift of 3 μm. The contribution from the uncertainty on the detector alignment is estimated by reconstructing the B_s^0 candidate events with the position of the SMT sensors shifted radially outwards by the alignment error in the radial position of the sensors. The resulting difference in fitted proper decay length of 2 μm is taken as the systematic uncertainty due to possible misalignment. The total systematic uncertainty from all these sources added in quadrature is 6 μm. The systematic uncertainties in the measurement of the $c\tau(B^0)$ are determined in the same way as for the B_s^0, and each contribution is listed in Table II.

TABLE II: Summary of systematic uncertainties.

	$c\tau(B_s^0)$ (μm)	$c\tau(B^0)$ (μm)	$\tau(B_s^0)/\tau(B^0)$
Alignment	2	2	0.000
J/ψ vertex	3	4	0.002
Model for resolution	3	3	0.000
Background	4	5	0.002
Total	**6**	**7**	**0.003**

We determine the lifetimes of the B_s^0 and B^0 mesons,

$$\tau(B_s^0) = 1.444^{+0.098}_{-0.090}\ (\text{stat})\ \pm 0.020\ (\text{sys})\ \text{ps},$$

$$\tau(B^0) = 1.473^{+0.052}_{-0.050}\ (\text{stat}) \pm 0.023\ (\text{sys})\ \text{ps}.$$

Both results are consistent with the current world averages of $\tau(B_s^0) = 1.461 \pm 0.057$ ps and $\tau(B^0) = 1.536 \pm 0.014$ ps [2]. We note that measurements using B_s^0 semileptonic events, where there is an equal mixture of *CP*-even and *CP*-odd states, dominate the current world average, while $B_s^0 \to J/\psi\phi$ has a different composition of *CP*-even and *CP*-odd states as discussed earlier [6].

Using our results we determine the ratio of B_s^0/B^0 lifetimes to be

$$\frac{\tau(B_s^0)}{\tau(B^0)} = 0.980\ ^{+0.076}_{-0.071}\ (\text{stat})\ \pm 0.003\ (\text{sys}),$$

where statistical uncertainties were propagated in quadrature, and the systematic uncertainty was evaluated by adding each contribution to the corresponding central value, and evaluating a new ratio, with the difference from the nominal value taken as the systematic uncertainty of that source, as shown in Table II. The sum in quadrature of all contributions is reported as the overall systematic uncertainty on the ratio of lifetimes including correlations between the two lifetime measurements.

In conclusion, we have measured the B_s^0 and B^0 lifetimes in exclusive decay modes in $p\bar{p}$ collisions. The measurements are consistent with previous results [2]. The value of the B_s^0 lifetime obtained in this analysis is the most precise measurement from any single experiment. The ratio of the lifetimes is also in good agreement with QCD models based on a heavy quark expansion, which predict a difference between B_s^0 and B^0 lifetimes of the order of 1% [1].

We thank the staffs at Fermilab and collaborating institutions, and acknowledge support from the Department of Energy and National Science Foundation (USA), Commissariat à l'Energie Atomique and CNRS/Institut National de Physique Nucléaire et de Physique des Particules (France), Ministry of Education and Science, Agency for Atomic Energy and RF President Grants Program (Russia), CAPES, CNPq, FAPERJ, FAPESP and FUNDUNESP (Brazil), Departments of Atomic Energy and Science and Technology (India), Colciencias (Colombia), CONACyT (Mexico), KRF (Korea), CONICET and UBACyT (Argentina), The Foundation for Fundamental Research on Matter (The Netherlands), PPARC (United Kingdom), Ministry of Education (Czech Republic), Natural Sciences and Engineering Research Council and WestGrid Project (Canada), BMBF and DFG (Germany), A.P. Sloan Foundation, Civilian Research and Development Foundation, Research Corporation, Texas Advanced Research Program, and the Alexander von Humboldt Foundation.

[*] Visitor from University of Zurich, Zurich, Switzerland.
[†] Visitor from Institute of Nuclear Physics, Krakow, Poland.

[1] M. B. Voloshin and M. A. Shifman, Sov. Phys. JETP **64**, 698 (1986); I. Bigi and N. G. Uraltsev, Phys. Lett. B **280**, 271 (1992); I. Bigi, Nuovo Cimento A **109**, 713 (1996); F. Gabbiani, A. I. Onishchenko and A. A. Petrov, arXiv:hep-ph/0407004.
[2] S. Eidelman *et al.* (Particle Data Group), Phys. Lett. B **592**, 1 (2004).
[3] I. Bigi *et al.* in "B Decays", 2nd edition, edited by S. Stone, (World Scientific, Singapore 1994) p. 13 ; I. Dunietz, Phys. Rev. D **52**, 3048 (1995); M. Beneke, G. Buchalla, I. Dunietz, Phys. Rev. D **54**, 4419 (1996).
[4] T. LeCompte and H. T. Diehl, "The CDF and DØ Upgrades for Run II", Ann. Rev. Nucl. Part. Sci. **50**, 71 (2000); V. Abazov, *et al.*, in preparation for submission to Nucl. Instrum. Methods Phys. Res. A.
[5] J. Abdallah *et al.* (DELPHI Collaboration), Eur. Phys. J. C **32**, 185 (2004).
[6] The exact fraction of *CP*-even and *CP*-odd decays is un-

known. In this analysis, from Monte Carlo, the relative efficiency for CP-even and CP-odd states is 0.99 ± 0.01.

APPENDIX: B^0 MASS DISTRIBUTIONS

Figure 3 shows the invariant mass distributions for reconstructed B^0 candidates before and after the $c\tau$ cut.

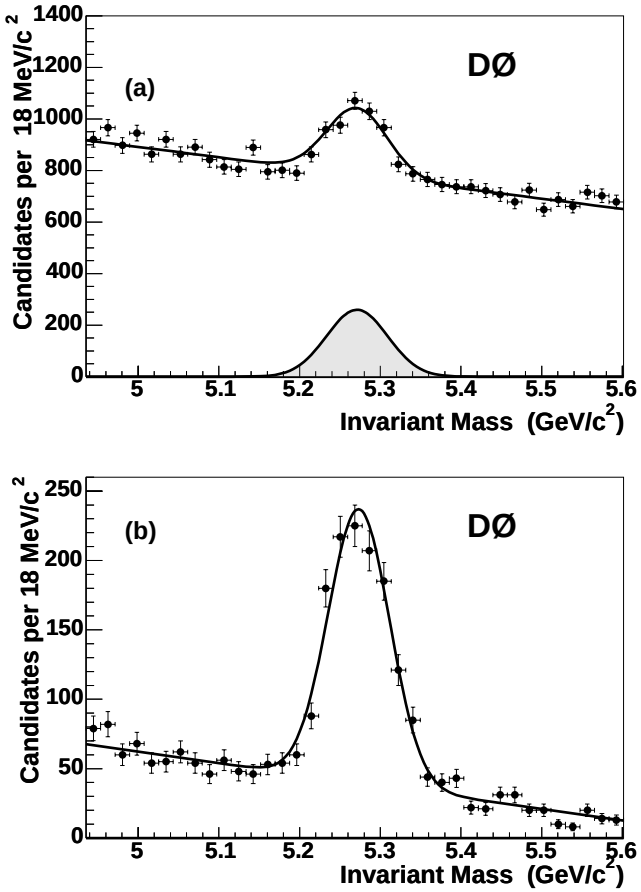

FIG. 3: (a) Mass distribution for B^0 candidate events. Points with error bars show the data, and the solid curve represents the result of the fit. The mass distribution for the signal is shown in gray; (b) same distribution after requiring the significance of the lifetime measurement to be $c\tau/\sigma(c\tau) > 5$.